Angle-domain Migration Velocity Analysis using Wave-equation Reflection Traveltime Inversion

Sanzong Zhang, Gerard Schuster, King Abdullah University of Science and Technology, and Yi Luo, Saudi Aramco*

SUMMARY

The main difficulty with an iterative waveform inversion is that it tends to get stuck in a local minima associated with the waveform misfit function. This is because the waveform misfit function is highly non-linear with respect to changes in the velocity model. To reduce this nonlinearity, we present a reflection traveltime tomography method based on the wave equation which enjoys a more quasi-linear relationship between the model and the data. A local crosscorrelation of the windowed downgoing direct wave and the upgoing reflection wave at the image point yields the lag time that maximizes the correlation. This lag time represents the reflection traveltime residual that is back-projected into the earth model to update the velocity in the same way as wave-equation transmission traveltime inversion. The residual movemout analysis in the angle-domain common image gathers provides a robust estimate of the depth residual which is converted to the reflection traveltime residual for the velocity inversion. We present numerical examples to demonstrate its efficiency in inverting seismic data for complex velocity model.

INTRODUCTION

Prestack depth migration of 3D seismic data is the industry standard for computing detailed estimates of the earth's reflectivity distribution. However, an accurate velocity model is a precondition for accurately imaging complex geological structures. Migration velocity analysis (MVA) is the most popular method to robustly estimate the velocity model with a complex geology. It selects the optimal migration velocity as the one that best flattens the reflection CIGs.

There are usually two different implementations for MVA: traveltime inversion and wave-equation inversion. For traveltime inversion (Bishop et al., 1985; Al-Yahya, 1989; Stork and Clayton, 1991; Stork, 1992), the reflection traveltime residuals are smeared along the ray path to invert for smooth features of the velocity model, while wave-equation inversion smears the image-related perturbation along the wavepath for fine details of the earth model (Biondi and Sava, 1999; Mulder and Kroode, 2002; Sava and Biondi, 2004a and 2004b; Soubaras and Gratacos, 2007; Xie and Yang, 2008; Shen and Symes, 2008). Ray-based traveltime inversion is constrained by a high-frequency approximation, and so it fails to invert for the earth's velocity variations having nearly the same wavelength or less than that of the source wavelet. Consequently, the resolution of the velocity model constructed from ray-based traveltime inversion is much less than that of wave-equation inversion. The ray-based method may become unreliable when the multipath problem exists due to complex geology. The merit is that the traveltime misfit function is quasi-linear with respect to velocity perturbations so that an efficient velocity inversion can be achieved even if the starting model is far from the actual model (Luo and Schuster, 1991a and 1991b; Zhou et al., 1995).

Although very sensitive to the choice of starting models or noisy amplitudes, wave-equation inversion can, in principle, reconstruct a finely detailed estimate of the earth model because there is no high-frequency assumption. The problem with wave-equation inversion, however, is that its misfit function can be highly nonlinear with respect to changes in the velocity model. In this case, a gradient method will tend to get stuck in a local minima if the starting model is far away from the actual model. Nevertheless, wave-equation inversion is more accurate in modeling waves in complex subsurface regions.

To exploit the strengths and ameliorate the weaknesses of both ray-based traveltime inversion and wave-equation inversion, wave-equation-based traveltime inversion was developed to invert the velocity model (Luo and Schuster, 1991a and 1991b; Zhang and Wang, 2009; Zhou et al, 1995; Leeuwen and Mulder, 2010). This kind of inversion methods inverts traveltimes using the gradient calculated from the wave equation. It is not constrained by a high-frequency approximation. Other important benefits are a convergence rate that is somewhat insensitive to the starting model, a high degree of model resolution, and a robustness in the presence of data noise. However, these traveltime inversion methods are designed to invert transmission, not reflection, waves in seismic data. Unlike refraction and direct waves, reflections can provide more velocity information in the deeper subsurface for model inversion. Wave-equation reflection traveltime inversion (Zhang et al., 2011) is proposed to invert reflection traveltimes to estimate the velocity model. The key ideal of this method is that a local cross-correlation of the windowed downgoing direct wave and the upgoing reflection wave at the image point yields the lag time that maximizes the correlation. This lag time represents the reflection traveltime residual that is back-projected into the earth model to update the velocity in the same way as wave-equation transmission traveltime inversion.

A convenient data type for implementation of wave-equation reflection traveltime inversion is with commom image gathers(CIGs). CIGs are generally employed to measure the accuracy of the velocity model in migration velocity analysis. The correct velocity model flattens all events in CIGs, whereas an inaccurate velocity model generates curved events. Their curvature can be used to update the velocity model which is often done in offset-domain CIGs. However, surface-related CIGs suffer from migration artifacts due to multipath of wave propagation and can lead to erroneous results for MVA. Angle-domain CIGs are proposed to eliminate artifacts present in offset-domain or shot-domain CIGs (Xu et al., 2001; Xu et al., 2011). This is compared to Zhang et al.(2011) who estimate reflection traveltime residuals by correlating extrapolated data traces, and then update the velocity by smearing them along

DOI http://dx.doi.org/10.1190/segam2012-1123.1

the reflection wavepaths. This procedure works well for mild complexity in the velocity model, but become less reliable for complex velocity models. To alleviate this problem, we estimate the traveltime residual in angle-domain CIGs. That is, we now conduct the residual movemout analysis in angle-domain CIGs to estimate the depth residuals and then convert the depth residual to the time residual for wave-equation reflecton traveltime inversion.

This paper is organized into four sections. The first section describes the basic theory of wave-equation reflection traveltime inversion. The second section presents the theory for angle-domain MVA, including a description of the angle-domain CIGs decomposition and residual moveout analysis. The third section shows a numerical example to verify the effectiveness of this method, and the last section draws some conclusions

THEORY

Wave-equation reflection traveltime inversion

The sensitivity kernel of wave-equation reflection traveltime inversion (Zhang et al., 2011) is

$$\gamma(\mathbf{x}') = \gamma_1(\mathbf{x}') + \gamma_2(\mathbf{x}') \tag{1}$$

$$\gamma_1(\mathbf{x}') = \frac{2}{c(\mathbf{x}')^3} \sum_{\mathbf{s}} \sum_{\mathbf{x}} \int \overbrace{\left[\dot{p}(\mathbf{x}', t+\Delta\tau|\mathbf{x}_s)_{cal} \right]}^{\text{Forward prop. of the source}} \overbrace{\left[\frac{\Delta\tau}{E} p_g(\mathbf{x},t) * \ddot{g}(\mathbf{x}', -t|\mathbf{x},0) \right]}^{\text{Backprop. of the redatumed data}} dt \tag{2}$$

$$\gamma_2(\mathbf{x}') = \frac{2}{c(\mathbf{x}')^3} \sum_{\mathbf{s}} \sum_{\mathbf{x}} \int \overbrace{\left[\dot{p}(\mathbf{x}, t+\Delta\tau|\mathbf{x}_s)_{cal} * \dot{g}(\mathbf{x}', t|\mathbf{x},0) \right]}^{\text{Forward prop. of the redatumed source}} \overbrace{\left[\int \frac{\Delta\tau}{E} p(\mathbf{x}_g, t|\mathbf{x}_s)_{obs} * \dot{g}(\mathbf{x}', -t|\mathbf{x}_g,0) d\mathbf{x}_g \right]}^{\text{Backprop. of the observed data}} dt, \tag{3}$$

where $\mathbf{s}$ is the source, $\mathbf{x}$ is at the trial image point, $\Delta\tau$ is the reflection traveltime residual in the trial image point, $\gamma(\mathbf{x}')$ represents the traveltime misfit gradient at $\mathbf{x}'$, $p(\mathbf{x}_r, t|\mathbf{x}_s)_{cal}$ denotes the calculated seismogram, $p(\mathbf{x}_r, t|\mathbf{x}_s)_{obs}$ denotes the observed data, $p_g(\mathbf{x},t)$ is the redatumed data and $g(\mathbf{x}_r, t|\mathbf{x}_s)$ is the Green function.

From the above equation, we can see that the gradient of the wave-equation reflection traveltime inversion consists of two terms. Both of them can be treated as the misfit gradient of wave-equation transmission traveltime inversion:

1). The first term ($\gamma_1(\mathbf{x}')$) can be treated as the misfit gradient of wave-equation transmission traveltime inversion by redatuming the observed data from the surface to the reflectors. For a single source, the interpretation of this term is that the forward modeled field $\dot{p}(\mathbf{x}', t+\Delta\tau|\mathbf{x}_s)_{cal}$ is crosscorrelated with the back-propagated field $p_g(\mathbf{x},t) * \ddot{g}(\mathbf{x}', -t|\mathbf{x},0)$ to yield the gradient value at $\mathbf{x}'$. The back-propagated field is found by back-propagating the pseudo traveltime residual which is formed by weighting the redatumed seismic reflection event at the reflector $\mathbf{x}$ with its associated traveltime residual $\Delta\tau$ and the normalization value E.

2). The second term ($\gamma_2(\mathbf{x}')$) can be treated as the misfit gradient of wave-equation transmission inversion by redatuming the source to the reflectors. The interpretation of this term is that the forward modeled field $\dot{p}(\mathbf{x}, t+\Delta\tau|\mathbf{x}_s)_{cal} * g(\mathbf{x}', t|\mathbf{x},0)$ is cross-correlated with the back-propagated field $p(\mathbf{x}_g, t|\mathbf{x}_s)_{obs} * g(\mathbf{x}', -t|\mathbf{x}_g,0)$ to yield the gradient value at $\mathbf{x}'$. The forward modeling field is obtained by redatuming the source at $\mathbf{x}_s$ to the reflector at $\mathbf{x}$, and then forward propagating the redatumed source at the reflector $\mathbf{x}$ to $\mathbf{x}'$. The back-propagated field is found by back-propagating the pseudo traveltime residual which is formed by weighting the observed seismic reflection event $p(\mathbf{x}_g, t|\mathbf{x}_s)_{obs}$ with its associated traveltime residual $\Delta\tau$ and the normalization value E.

Figure 1 illustrates the essential elements of this method for a two-layer model. The common shot gathers recorded by the surface geophones are displayed in Figure 1b, and the reflection wavepath of is shown in Figure 1d.

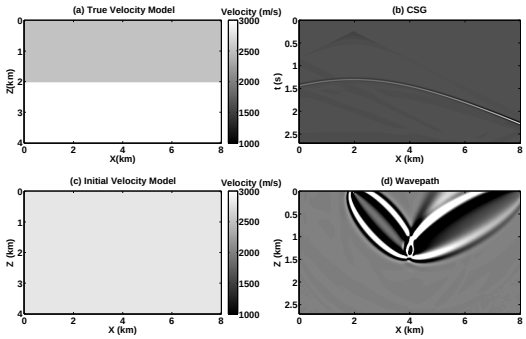

Figure 1: (a). Two-layer velocity model. (b). One common shot gather. (c). The initial velocity model. (d). The senstivity kernel of wave-equation reflection traveltime inversion.

Conversion from depth residual to time residual

For complex velocity models, the crosscorrelation function has maxima at many lag values. To find the optimal lag values associated with the misfit between a predicted and observed reflection traveltime, we employ a robust method to estimate the time shift by converting the depth residual to the time residual in the angle-domain CIGs. The relationship between the depth residual and the time residual (Sava and Fomel, 2006) is

$$\Delta\tau = s\cos\theta\cos\alpha\Delta z. \tag{4}$$

where $\Delta\tau$ is the time shift, Δz is the depth shift, s is the slowness, α is the dip angle of reflectors and θ is the reflection

DOI http://dx.doi.org/10.1190/segam2012-1123.1

angle. From equation (4), we can see that the reflection angle θ, the dip angle of reflector α, and the depth residual Δz must be known in order to convert the depth shift Δz to the time shift $\Delta\tau$. The dip angle of reflectors equates the normal direction of reflectors with respect to the vertical direction. One way of computing the dip angle or normal angle of reflectors is to use the structural tensor approach. In this paper we use the weighted structural tensor approach to calculate the dip angle from the migration image (Luo et al., 2006). The reflection angle at the image point is the difference between the incidence wave propagation angle β and the normal angle of reflectors, and both are computed with respect to the vertical direction.

$$\theta = \beta - \alpha \tag{5}$$

In 2D, the wave propagation angle (Zhang and McMechan, 2010) is

$$\beta = \tan^{-1}\left[\frac{\partial p}{\partial x}\Big/\frac{\partial p}{\partial z}\right] \tag{6}$$

Angle-domain CIGs and moveout analysis

The angle-domain CIG provides a new opportunity for migration velocity analysis since it is less sensitive to migration artifacts in the presence of the multiples (Xu et al., 2001; Xu et al., 2011). There are several types of angle-domain CIGs decomposition methods available now. Here we adapt the method proposed by Sava and Fomel (2003) which outputs the local subsurface-offset CIGs from one-way or two-way wave equation migration. These CIGs are converted to the subsurface reflection angle-domain CIGs by a slant stack method.

There are several steps for the residual movemout analysis.
1). The migration imaging condition is applied at a range of subsurface offsets, forming subsurface-offset CIGs.
2). A 2D Fourier transform is applied to the local offset CIG to form angle-domain CIGs by mapping the wavenumber to the reflection angle eventually.
3). Assuming the velocity model is uniform, a typical residual curvature moveout of angle-domain CIGs (Biobdi and Symes, 2004) is expressed as

$$z^2 = z_0^2 + \gamma(z_0 \tan\theta)^2, \tag{7}$$

where z is the depth, z_0 is the reference zero angle depth of one reflection event in angle-domain CIGs and γ is the coefficient related to curvature. This equation is used to conduct the semblance analysis in the angle-domain CIGs.
4). The depth residual can be obtained by

$$\Delta z = z - z_0. \tag{8}$$

Figure 2 shows an example to illustrate the moveout analysis in angle-domain CIGs. The inaccuracy of the migration image can be measured clearly in the angle-domain CIGs in Figure 2a. The curved events in the angle-domain CIGs indicate the inaccuracy of the migration velocity model. The moveout analysis uses equation (7) to fit the events in the angle-domain CIGs. The local maxmimum in the semblance panel in Figure 2 represents z_0 and γ which can be automatically or manually picked in practice. Each maxmum represents a curve in angle-domain CIGs denoted by the blue line in Figure 2a.

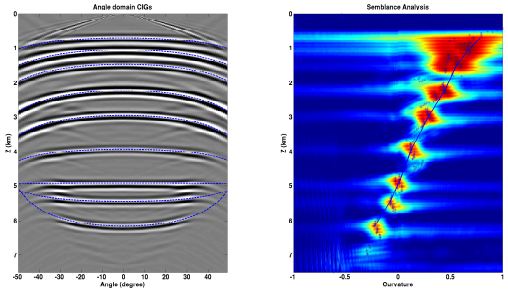

Figure 2: (a). Angel-domain CIGs. (b). Semblance analysis panel. The blue dashed line in (a) represents the moveout of reflection events. The blue line in (b) indicates the maximum in the semblance panel.

NUMERICAL EXAMPLES

Figure 3b shows the synthetic seismograms generated by a fourth-order finite-difference solution to the 2-D acoustic wave equation (with constant density). The model in Figure 3a is discretized into a mesh with 375x909 grid points, with 181 line sources and 523 receivers on the top surface of the model, respectively. A 40-gridpoint wide absorbing sponge zone is added along each boundary. The grid interval is 20 meters, the source wavelet is a Ricker wavelet with a peak frequency of 15 Hz, and the starting velocity model is shown in Figure 4a. Figure 4b shows the inverted velocity model after 15 iterations. The angle-domain MVA using wave-equation reflection traveltime inversion reconstructs the velocity model correctly, especially in the deep parts of the model. Figure 5 shows the reverse time migration images using the initial velocity model and the inverted velocity model. The difference between these two images is obvious in the location and the coherence of the deep reflectors. These reflection events become flat in the angle-domain CIGs calculated from the inverted velocity model in Figure 6b. It is further verified that the inverted velocity model is more accurate than the initial velocity model for reverse time migration.

CONCLUSION

This paper presents a new method for angle-domain MVA. The key ideal is to apply wave-equation reflection traveltime inversion to traveltime residuals estimated in the angle-domain CIGs. Compared to the conventional ray-based offset domain (or shot-domain) MVA, this method does not suffer from a high-frequency approximation and can be used for the complex velocity model building. The moveout analysis in the angle-domain CIGs provides a robust method to estimate the depth shift which can be converted into the time shifts. The numerical example illustrates its effectiveness in velocity model building. However, the weakness if this method for complex velocity model is that starting velocity model must be accurate enough so as to render a CIG with coherent reflection events. The future research will apply this method to complex velocity model.

DOI http://dx.doi.org/10.1190/segam2012-1123.1

ACKNOWLEDGMENTS

We thank the 2012 sponsors of Center for Subsurface Imaging and Fluid Modeling (CSIM) at KAUST for their support (http://csim.kaust.edu.sa).

REFERENCES

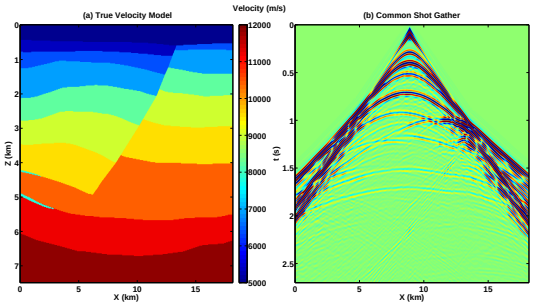

Figure 3: (a). True velocity model. (b). Common shot gathers.

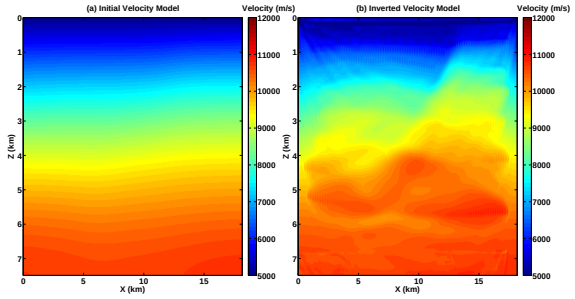

Figure 4: (a). Initial velocity model. (b). Inverted velocity model.

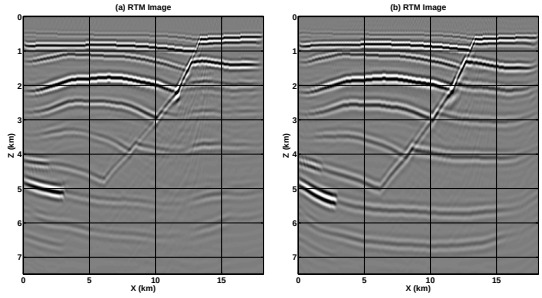

Figure 5: (a). The reverse time migration image using the initial velocity model in Figure 4a. (b). The reverse time migration image using the inverted velocity model in Figure 4b.

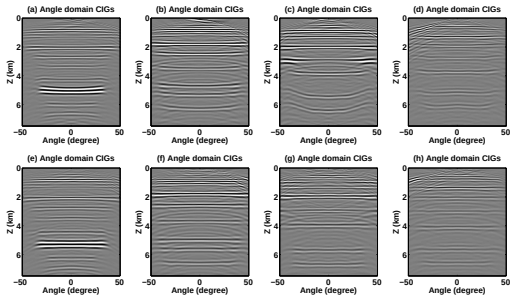

Figure 6: The angle-domain CIGs. The first row is the angle-domain CIGs using the initial velocity mode in Figure 4a. The second row is the angle-domain CIGs using the true velocity model in Figure 4b.

DOI http://dx.doi.org/10.1190/segam2012-1123.1

http://dx.doi.org/10.1190/segam2012-1123.1

EDITED REFERENCES

Note: This reference list is a copy-edited version of the reference list submitted by the author. Reference lists for the 2012 SEG Technical Program Expanded Abstracts have been copy edited so that references provided with the online metadata for each paper will achieve a high degree of linking to cited sources that appear on the Web.

REFERENCES

Al-Yahya, K., 1989, Velocity analysis by iterative profile migration: Geophysics, **54**, 718–729.

Biondi, B., and P. Sava, 1999, Wave-equation migration velocity analysis: 69th Annual International meeting, SEG, Expanded Abstracts, 1723–1726.

Biondi, B., and W. Symes, 2004, Angle-domain common-image gathers for migration velocity analysis by wavefield-continuation imaging: Geophysics, **69**, 1283–1298.

Bishop, T., K. Bube, R. Cutler, R. Langan, P. Love, J. Resnick, R. Shuey, D. Spindler, and H. Wyld, 1985, Tomographic determination of velocity and depth in laterally varying media: Geophysics, **50**, 903–923.

Leeuwen, T., and W. Mulder, 2010, A correlation-based misfit criterion for wave-equation traveltime tomography: Geophysical Journal International, **182**, 1383–1394.

Luo, Y., and G. Schuster, 1991a, Wave equation traveltime inversion: Geophysics, **56**, 645–653.

Luo, Y., and G. Schuster, 1991b, Wave equation inversion of skeletonized geophysical data: Geophysical Journal International, **105**, 289–294.

Luo, Y., Y. Wang, N. AlBinHassan, and M. Alfaraj, 2006, Computation of dips and azimuths with weighted structural tensor approach: Geophysics, **71**, no. 5, V119–V121.

Mulder, W., and A. Kroode, 2002, Automatic velocity analysis by differential semblance optimization: Geophysics, **67**, 1184–1191.

Sava, P., and B. Biondi, 2004a, Wave-equation migration velocity analysis: Part 1: Theory: Geophysical Prospecting, **52**, 593–606.

Sava, P., and B. Biondi, 2004b, Wave-equation migration velocity analysis: Part 2: Subsalt imaging examples: Geophysical Prospecting, **52**, 607–623.

Sava, P., and S. Fomel, 2003, Angle-domain common-image gathers by wavefield continuation methods, Geophysics: **68**, 1065–1074.

Sava, P., and S. Fomel, 2006, Time-shift imaging condition in seismic migration: Geophysics, **71**, no. 6, S209–S217.

Shen, P., and H. Calandra, 2005, One-way waveform inversion within the framework of adjoint state differential migration: 75th Annual International Meeting, SEG, Expanded Abstracts, 1709–1712.

Shen, P., and W. Symes, 2008, Automatic velocity analysis via shot profile migration: Geophysics, **73**, no. 5, VE49–VE59.

Soubaras, R., and B. Gratacos, 2007, Velocity model building by semblance maximization of modulated-shot gathers: Geophysics, **72**, no. 5, U67–U73.

Stork, C., 1992, Reflection tomography in the postmigrated domain: Geophysics, **57**, 680–692.

Stork, C., and R. W. Clayton, 1991, An implementation of tomographic velocity analysis: Geophysics, **56**, 483–495.

Symes, W., and M. Kern, 1994, Inversion of reflection seismograms by differential semblance analysis: Algorithm structure and synthetic examples: Geophysical Prospecting, **42**, 565–614.

Wang, B., C. Mason, M. Guo, K. Yoon, J. Cai, J. Ji, and Z. Li, 2009, Subsalt velocity update and composite imaging using reverse-time-migration based delayed-imaging-time scan: Geophysics, **74**, no. 6, WCA159–WCA167.

Xie, X., and H. Yang, 2008, The finite-frequency sensitivity kernel for migration residual moveout and its applications in migration velocity analysis: Geophysics, **73**, S241–S249.

Xu, S., H. Chauris, G. Lambaré, and M. Noble, 2001, Common-angle migration: A strategy for imaging complex media: Geophysics, **66**, 1877–1894.

Xu, S., Y. Zhang, and B. Tang, 2011, 3D angle gathers from reverse time migration: Geophysics, **76**, no. 2, S77–S92.

Zhang, S., G. Schuster, and Y. Luo, 2011, Wave-equation reflection traveltime inversion: 81st Annual International Meeting, SEG, Expanded Abstracts, 2705–2710.

Zhang, Q., and G. McMechan, 2010, Direct vector-field method to obtain angle-domain common-image gathers from isotropic acoustic and elastic reverse time migration: Geophysics, **76**, no. 5, WB135–WB149.

Zhang, Y., and D. Wang, 2009, Traveltime information-based wave-equation inversion: Geophysics, **74**, no. 6, WCC27–WCC36.

Zhou, C., W. Cai, Y. Luo, G. Schuster, and S. Hassanzadeh, 1995, Acoustic wave-equation traveltime and waveform inversion of crosshole seismic data: Geophysics: **60**, 765–773.